JACS
JOURNAL OF THE AMERICAN CHEMICAL SOCIETY
Article
pubs.acs.org/JACS

Uptake of SO_2 to Aqueous Formaldehyde Surfaces

Stephanie T. Ota and Geraldine L. Richmond*

Department of Chemistry, University of Oregon, Eugene, Oregon 97403, United States

ABSTRACT: Aqueous surfaces act as a gateway to absorption and aqueous-phase reaction of gases in the atmosphere. The composition of aerosols varies greatly and is expected to influence the structure of the interface. For example, aldehydes comprise a significant fraction of atmospheric organics and are likely to accumulate at aqueous surfaces. But it is difficult to anticipate their effect on the migration of gaseous species through the interfacial region. Surface organics may act as a barrier to absorption, or they may facilitate uptake via cooperative interactions with absorbing compounds. The surface spectroscopic studies presented here examine the nature of the vapor/water interface during uptake of SO_2 to aqueous formaldehyde solutions, elucidating the role of surface species in a multicomponent interfacial system. The results show that the product of the reaction between SO_2 and formaldehyde, hydroxymethanesulfonate, shows a surface affinity that is enhanced in the presence of SO_2.

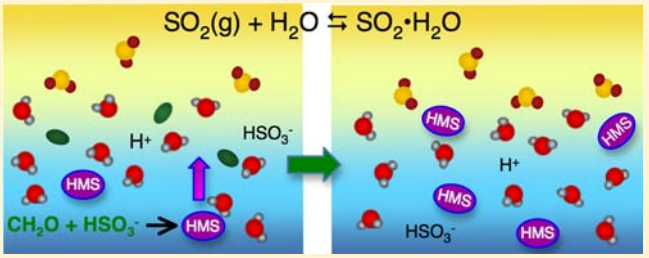

INTRODUCTION

Formaldehyde (CH_2O) and sulfur dioxide (SO_2) are gaseous pollutants with both natural and industrial sources. These primary pollutants can accumulate in fogwater and cloud droplets, and they play an important role in the formation of secondary pollutants such as sulfates, organosulfates, and organic aerosols in the atmosphere.[1−8] Aerosol particles in urban environments decrease air quality, which can lead to health problems, and persistent organic aerosols are predicted to have important implications for both global and regional climate change.[9−28] As scientists continue to learn about the behavior of pollutant species in the atmosphere, persistent questions remain about the role of the interface in determining the lifetime of aqueous aerosol particles. It is often difficult to extract information about interfacial behavior, as many techniques cannot distinguish surface contributions from those of the bulk. Thus, many of the gaps in our understanding of aerosol surface chemistry are related to the behavior and influence of organic constituents on interfacial behavior.[29−34] For example, how do organic solutes influence interfacial adsorption probabilities and reactivity at aqueous surfaces?

In the work presented here, the surface specificity of vibrational sum frequency spectroscopy (VSFS) is utilized to illuminate the details of surface interactions in the uptake of SO_2 to aqueous CH_2O solutions. This work aims to understand the role that interfacial formaldehyde plays on the uptake, and subsequent reaction, of SO_2 gas at aqueous surfaces. In addition to its environmental relevance, SO_2 displays distinctive surface behavior upon adsorption to water. Previous work in this laboratory showed that SO_2 gas binds to water, forming a surface complex whose formation is enhanced at lower temperatures.[35−37]

Formaldehyde (CH_2O), a commonly used industrial chemical, is the most abundant carbonyl compound in the atmosphere.[38] Formaldehyde is highly soluble in water, where it reacts to form methylene glycol (MG):

$$H_2C{=}O + H_2O \rightleftharpoons HOCH_2OH \quad (1)$$

At CH_2O concentrations above 5 mol %, MG can also react to form longer oligomers.[39] For the ensuing discussion, formaldehyde (aq) or CH_2O (aq) will be used to refer to all solvated forms of formaldehyde, including MG and other oligomers that may be present. IR and Raman spectroscopy are commonly applied to probe the aqueous chemistry of formaldehyde,[40−44] while uptake studies, coupled with theoretical models, have also examined the probability of formaldehyde partitioning to water and ice surfaces.[3,4,6,38,45−50]

In addition to its reaction with water, formaldehyde reacts with aqueous SO_2 to form relatively stable sulfonic acid products in the following manner:[51,52]

$$CH_2O + HSO_3^- \rightleftharpoons HOCH_2SO_3^- \text{ (HMS)}$$
$$K_{eq} = 6.5 \times 10^3\ M^{-1} \text{ at pH } 2 \quad (2)$$

This reaction has important environmental implications, particularly with the recognition that organosulfate species are an important component of secondary organic aerosols.[8] Measurements of hydroxymethanesulfonate (HMS) in the fogwater and cloudwater of polluted areas indicate a correlation between high HMS concentration and high levels of formaldehyde and S(IV) species in the atmosphere.[53,54] In the absence of aldehydes, uptake of SO_2 to aqueous aerosol particles in the atmosphere often results in the formation of sulfuric acid, a major component of acid rain. Aqueous sulfuric acid forms after SO_2 reacts with water to form bisulfite

Received: December 13, 2011
Published: May 22, 2012

   dx.doi.org/10.1021/ja211632r | J. Am. Chem. Soc. 2012, 134, 9967−9977

(HSO_3^-) and sulfite (SO_3^{2-}) ions (S(IV)), which are readily oxidized by peroxides and ozone to form sulfates (S(VI)).

In contrast to HSO_3^- and SO_3^{2-}, HMS is stable against oxidation by hydrogen peroxide, a primary oxidant in aqueous aerosols.[52] It has been suggested that the formation of aldehyde−sulfite adducts in cloudwater and fogwater particles could account for up to a 2-fold increase in wet deposition of SO_2,[55] and that such particles may act as a vehicle for long-range transport of S(IV) species in the atmosphere, reducing the rates of S(VI) formation.[52,54,56−58]

Previous mass accommodation studies have examined the uptake of CH_2O gas onto aqueous particles as a function of pH and sulfite content.[45,46,49] The results indicated that surface complexation between formaldehyde and water may occur at low pH,[45] but uptake rates for aqueous SO_3^{2-} solutions found no indication of surface complexation.[49] These studies mainly focussed on the uptake of CH_2O to aqueous surfaces at neutral or alkaline pH and did not examine the reverse interaction, the uptake of SO_2 to aqueous formaldehyde.

In the vibrational studies presented in this work, we observe that aqueous formaldehyde accumulates at the surface, and that the surface population increases with bulk concentration. Building on this observation, we examine how the presence of this reactive organic compound influences the uptake behavior of SO_2 gas. The effects of formaldehyde on the structure of the neat vapor/water interface are presented first. This is followed by an examination of the effects of SO_2 uptake on surface formaldehyde at room temperature and colder. Upon reaction, HMS is found to migrate to the surface. Examinations of HMS surface behavior and its interactions with gas phase SO_2 provide new insights into gas−surface interactions in the presence of organics at the vapor/water interface.

BACKGROUND

Vibrational sum frequency spectroscopy is well suited to the study of aqueous interfaces. As a selective vibrational technique, VSFS provides insight into bond strength, orientation, and intermolecular interactions at surfaces, and there are many resources available on the general aspects of the technique.[59−82]

The sum-frequency intensity is proportional to the square of the second-order susceptibility, $\chi^{(2)}$, which has both resonant and nonresonant components (eq 3). Spectra are fit to deconvolve the individual resonant modes, a nontrivial task. Employing a fitting routine proposed by Bain[83] allows us to account for both the homogeneous and inhomogeneous line widths of the vibrational modes.

$$\chi^{(2)} = \chi^{(2)}_{NR}\, e^{i\psi} + \sum_{\nu} \int_{-\infty}^{+\infty} \frac{A_\nu\, e^{i\phi_\nu}\, e^{-[\omega_L - \omega_\nu/\Gamma_\nu]^2}}{\omega_L - \omega_{IR} + i\Gamma_L}\, d\omega_L \quad (3)$$

The first term, $\chi^{(2)}_{NR}$, in eq 3 is the nonresonant second-order susceptibilty. The second term, the resonant susceptibility, is a sum over all resonant vibrational modes and is represented $\chi^{(2)}_{R(\nu)}$. The resonant susceptibility, $\chi^{(2)}_{R(\nu)}$, is proportional to N, the number of molecules contributing to the sum frequency response, and $\langle\beta_\nu\rangle$, the orientationaly averaged molecular susceptibility:

$$\chi^{(2)}_{R(\nu)} = \frac{N}{\varepsilon_0}\langle\beta_\nu\rangle \quad (4)$$

The resonant susceptibility (eq 4) is fit as a convolution of the homogeneous line widths of the individual molecular transitions (half width at half-maximum, Γ_L) with inhomogeneous broadening (full width at half-maximum, $(2\ln 2\Gamma_\nu)^{1/2}$), as in the second term in eq 3. The transition strength A_ν is proportional to the product of the number of contributing molecules and their orientationally averaged IR and Raman transition probabilities. The frequencies of the IR, the Lorentzian, and the resonant modes are ω_{IR}, ω_L, and ω_ν, respectively. The phase of each resonant mode is φ_ν. Sum frequency spectral intensities are complex, and changes can arise from changes in the number of contributing molecules, changes in orientation, and/or changes in bond energies.

EXPERIMENTAL DETAILS

Laser System. The laser system used in these experiments has been described extensively in previous publications and will not be detailed here.[84−86] Briefly, sum frequency light is generated by overlapping 800 nm (∼2.6 ps, 1 kHz repetition rate) and tunable (2700−4000 cm^{-1}) infrared light in a co-propagating geometry at 56° and 67° from the surface normal, respectively. After filtering any reflected 800 nm light, the resultant sum frequency light is collected with a thermoelectrically cooled CCD camera (Princeton Instruments) in 3 cm^{-1} increments over the tunable range. All of the spectra presented and discussed here were taken using either the ssp- or sps-polarization schemes, in which the three letters denote the sum-frequency, visible, and infrared polarizations. Changing the polarization scheme from ssp to sps allows us to compare vibrational contributions resulting from a component of the dipole that is perpendicular or parallel to the interface, respectively, giving us insight into how specific molecules are oriented at the surface.

To minimize contamination, samples are poured into scrupulously clean glass dishes contained in a nitrogen-purged Kel-f cell fitted with CaF_2 windows. The Kel-f cell has three gas ports, two of which are used for gases, and the remaining port is vented via Teflon tubing to a fume hood. There is an additional port to accommodate the Teflon-coated Type T thermocouple probe used to monitor sample temperature. Data collection is facilitated using a Lab View program that selects the IR wavelength, records CCD intensity, and monitors the sample temperature for each data point.

Sample Preparation and Analysis. Gases were purchased from AirGas (nitrogen cylinder) and Air Liquide (SO_2, lecture bottle, 99.99%). Ten-milliliter ampules of 16% w/v (16 g of CH_2O/100 mL of H_2O) methanol-free formaldehyde were purchased from Fisher and diluted with high-purity water from a Barnstead E-pure system (18 MΩ) when necessary. Sum frequency intensities were measured using a thermoelectrically cooled CCD camera with a 2 s exposure time. Intensities were recorded in 3 cm^{-1} steps over a range from 2700 to 3900 cm^{-1}. Gas flow experiments were conducted at atmospheric pressure with a constant SO_2 gas flow rate of ∼10 sccm.

Sum frequency data are normalized to account for spatial variation between the visible and IR while scanning the IR frequency, temporal lengthening of IR pulses by water vapor, absorption of IR energy by SO_2 and/or water vapor, and the frequency dependence of the optics used for filtering the SF light. In these experiments, all SF spectra were divided by the nonresonant response from an uncoated gold surface. Spectra presented are averages of 3−12 spectra taken over multiple days to ensure reproducibility and to reduce the signal-to-noise ratio. Spectra of the neat vapor/water interface are taken at the beginning of each experiment, and spectral intensities are compared daily to ensure that the sum frequency response is comparable for each sample.

The parameters used to fit the neat vapor/water interface in ssp-polarization were established in previous isotopic dilution experiments.[87−89] Each resonant peak contains five variables (amplitude, vibrational frequency, Lorentzian and Gaussian widths, and phase (eq 3)); thus, there may be nonunique fitting solutions. To reduce the number of variables associated with the fits: The phases are fixed at either π (for peaks between 3200 and 3600 cm^{-1}) or 0 (for peaks below 3200 or above 3600 cm^{-1}); Lorentzian widths are fixed at either 12 cm^{-1} (for the free OH) or 5 cm^{-1} for the remaining OH stretches;

dx.doi.org/10.1021/ja211632r | J. Am. Chem. Soc. 2012, 134, 9967−9977

and with the exception of the free OH, Gaussian widths are broad (100−135 cm^{-1}). To constrain parameters, a global fitting routine is employed to iteratively fit the data while constraining peak positions and widths such that the only variables for different samples are the peak amplitudes, lending higher confidence to the results. Additional resonant peaks are added when they are both phenomenologically logical and necessary to achieve agreement between the data and the fits.

Spectral Analysis: The Neat Vapor/Water Interface. Water in the interfacial region occupies a wide range of molecular environments depending on orientation, hydrogen bonding and coordination to other molecules, and solvation of other species such as ions, and the sum frequency response from the OH stretching region is correspondingly broad. The lack of discrete spectral features can lead to ambiguity regarding the interpretation of VSFS data, and with continued research interpretations of interfacial water structure continue to evolve.[72,87,88,90−105] However, valuable information regarding interfacial behavior can still be inferred from examining spectral changes that occur when the aqueous surface is perturbed. To this end, a number of parameters have been defined to describe the spectroscopic response from the vapor/water interface. Support for this description of the VSFS data comes from previous isotopic dilution studies,[87,88,92] as well as from MD simulations[90,91] conducted in our laboratory, and supported by the work of others.[102−104]

Figure 1 shows a typical VSF response from vapor/water interface (black crosses) using the ssp-polarization scheme. The fitting

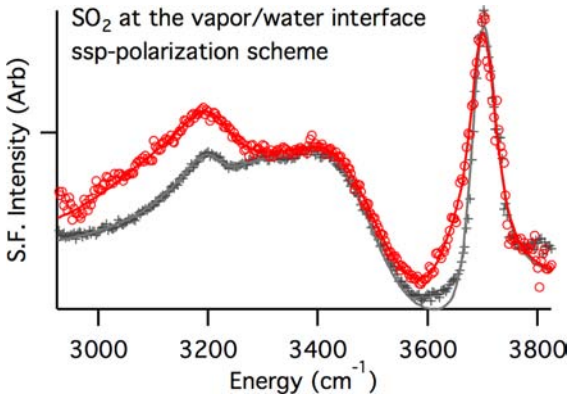

Figure 1. ssp-polarization spectrum of the vapor/water interface before (black crosses) and during (red circles) exposure to SO_2 at 23 °C. Solid lines are fits to the data.

parameters that will be applied in this study are as follows: (1) The sharp peak at ∼3700 cm^{-1} (the free OH) is attributed to unbound OH oscillators with an average orientation away from the bulk. This mode is highly sensitive to weakly bound species at the surface. (2) The mode opposite the free OH mode (the companion OH) points into the bulk and gives rise to broad spectral intensity at ∼3460 cm^{-1} consistent with measurements of the OH vibrations from uncoupled HOD in liquid water.[102] MD calculations supporting this assignment also indicate that such highly oriented water molecules interact weakly with neighboring molecules via hydrogen bonds through both the hydrogen and oxygen.[90,91,103] Loosely coupled water molecules in the more coordinated region of the interface also contribute to the intensity of this peak. (3) Much of the interfacial region is comprised of loosely bound water molecules nearly parallel to the interface, which are observed at ∼3580 cm^{-1} and contribute to the sps-polarization spectra.[91,103] (4) More coordinated water molecules, sometimes referred to as tetrahedrally bound water, reside deeper in the interfacial region and give rise to two modes at ∼3330 and ∼3200 cm^{-1}. While the molecular origins of the broad intensity in this region are not well understood, the consensus from isotopic dilution studies of the OD[99,100] and OH[87,88,92] stretching regions and recent MD simulations[91,93,101] is that the intensity increases with stronger hydrogen bonding and increased intermolecular coupling. With the exception of the peak at 3580 cm^{-1}, the ssp- and sps-polarization spectra are fit using the same peak parameters. Recent phase-sensitive experiments detect a phase shift below 3200 cm^{-1}, which is not accounted for in this description.[72,94−97] However, the signal amplitude from water in this frequency region is very low; thus, the use of an additional peak would be inconsequential for the overall interpretation.

Exposure to SO_2 (red circles) causes two primary changes to the spectral region, as shown in Figure 1: broadening of the free OH peak at 3700 cm^{-1}, and an increase in the region below 3500 cm^{-1} due to solvated ions and SO_2, as has been described in previous publications.[35−37] The broadening of the free OH peak is indicative of surface complexation between SO_2 and water and will be referred to frequently in the subsequent discussion.

RESULTS AND DISCUSSION

Formaldehyde at the Vapor/Water Interface. At 3.2% w/v formaldehyde, the bulk solution contains primarily methylene glycol ($CH_2(OH)_2$, or MG), but it is unknown whether the surface composition matches that of the bulk. In this work, the term formaldehyde(aq) will be used to refer to both MG and CH_2O. Figure 2 shows the ssp-polarization VSF

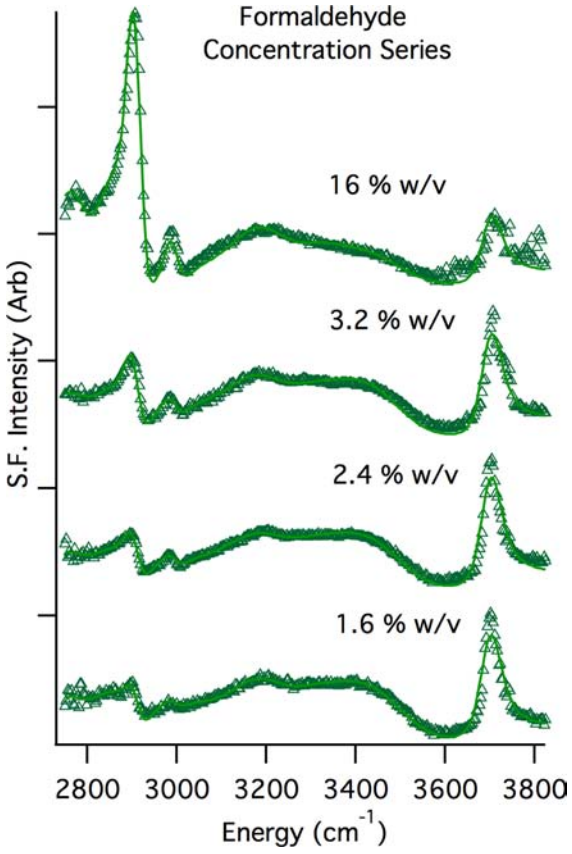

Figure 2. Global fits to ssp-polarization spectra of the vapor/CH_2O(aq) interface taken as a function of concentration. Solid lines are fits to the data.

spectral response, which probes vibrations with components normal to the surface, when the bulk concentration increases from 1.6 to 16% w/v formaldehyde. Figure 3 shows VSF spectra of 3.2% w/v formaldehyde (green plusses) at 23 (a,b) and 0 °C (c,d) using the (a,c) ssp- and (b,d) sps-polarization schemes. For reference, the neat vapor/water interface is shown as gray crosses. Notably, spectra obtained at ∼0 °C are nearly indistinguishable from those taken at room temperature. In the

dx.doi.org/10.1021/ja211632r | J. Am. Chem. Soc. 2012, 134, 9967−9977

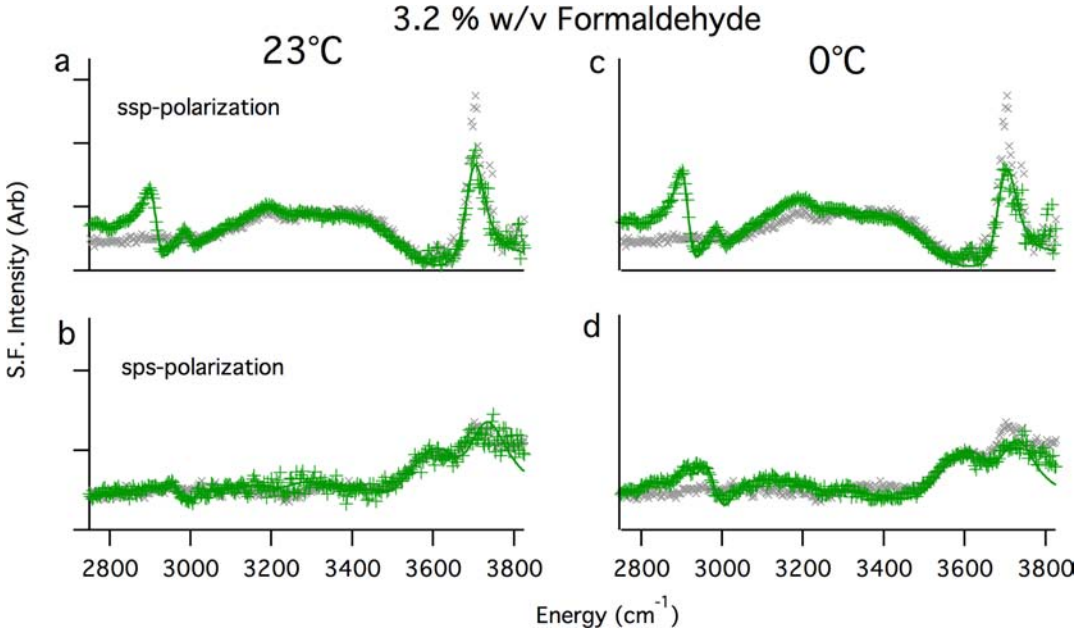

Figure 3. VSF spectra of 3.2% w/v formaldehyde (green pluses) at 23 (a,b) and 0 °C (c,d). Spectra were obtained in the (a,c) ssp- and (b,d) sps-polarization schemes. Water is shown as gray crosses for comparison. Solid lines are fits to the data.

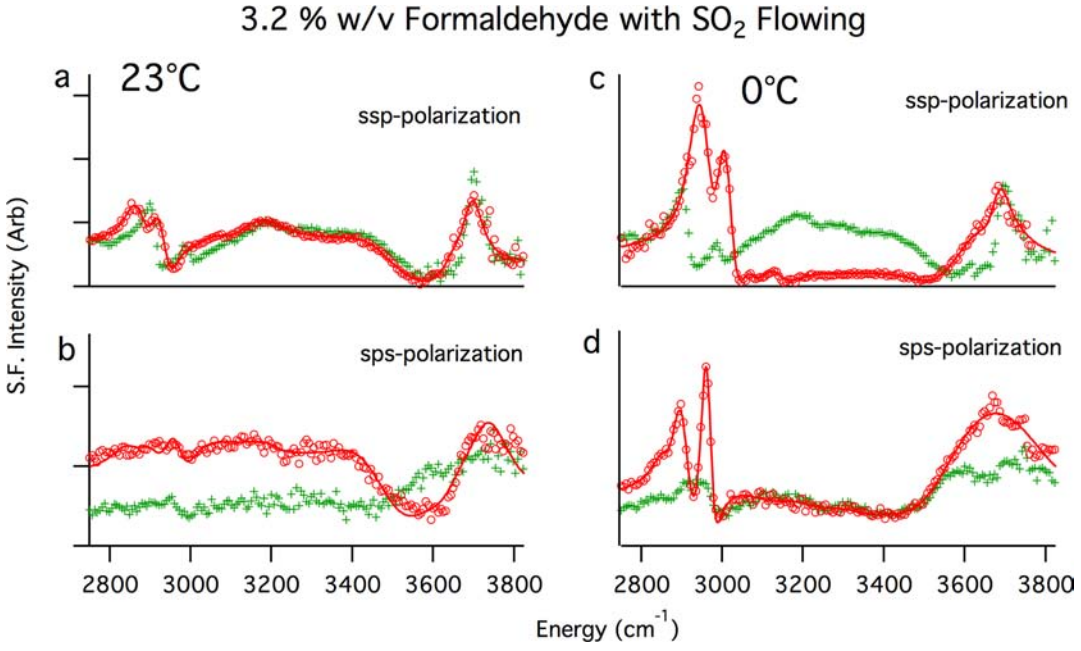

Figure 4. 3.2% w/v formaldehyde with SO_2 flowing (red) at 23 (a,b) and 0 °C (c,d). Spectra were taken using the (a,c) ssp- and (b,d) sps-polarization schemes. The vapor/formaldehyde interface is shown in green for reference. Solid lines are fits to data.

sps-polarization scheme (Figure 3d), the CH_2 peaks in the 2800−3000 cm^{-1} region are slightly more defined at 0 °C, but both solutions are fit using the same peak parameters. Adding formaldehyde to water results in two main spectral changes: in the water OH stretching region, contributions from loosely coordinated water molecules in the topmost surface region decrease, lowering the intensity of the peaks from the free and companion OH modes; new peaks, which are attributed to CH_2O(aq), appear in the CH stretching region below 3000 cm^{-1}.

Visual inspection of the data in Figures 2 and 3 indicates that formaldehyde(aq) is present at the aqueous surface, and that the surface concentration increases with increasing bulk concentration. Fits to the data in Figure 3 were obtained by initially allowing amplitudes and widths of the peak parameters for the neat vapor/water interface to vary to achieve a rough fit. Additional peaks were added as necessary to achieve agreement between the fits and the data. For added confidence in the fitting parameters, a global fit was performed for ssp-polarization spectra taken over a range of concentrations between 1.6 and 16% w/v formaldehyde (Figure 2). For formaldehyde, the best fits were achieved by incorporating two main peaks in addition to the standard four water modes: a broad peak at 3050 cm^{-1} and a sharp peak at 2910 cm^{-1}. In

dx.doi.org/10.1021/ja211632r | J. Am. Chem. Soc. 2012, 134, 9967−9977

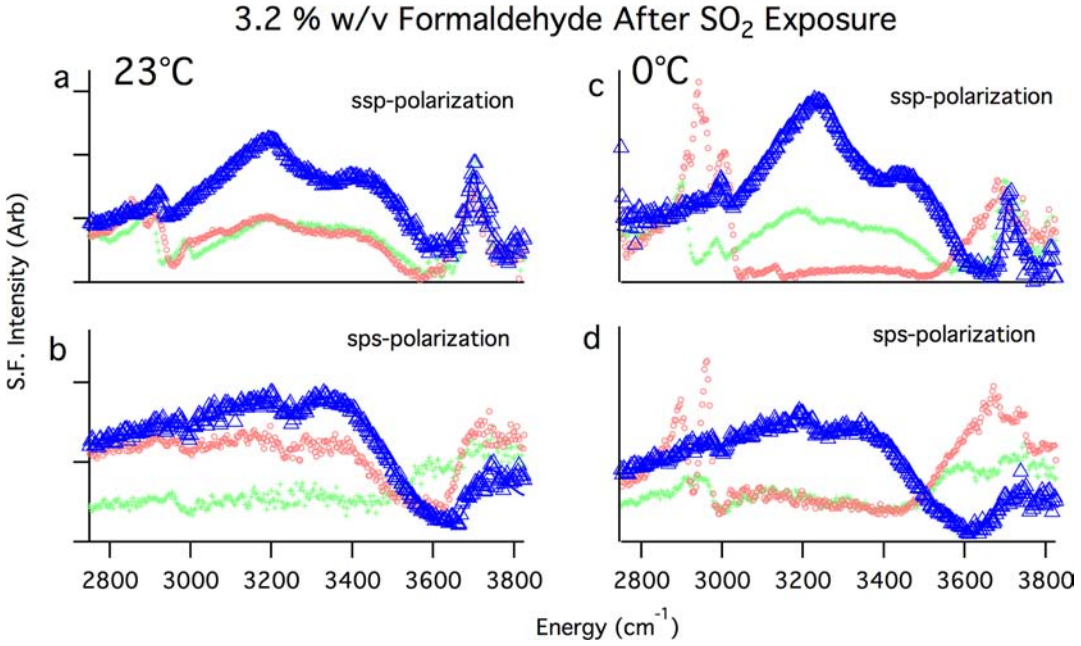

Figure 5. 3.2% w/v formaldehyde after exposure to SO_2 (blue triangles). Spectra were obtained at 23 (a,b) and 0 °C (c,d) in the (a,c) ssp- and (b,d) sps-polarization schemes. For reference, spectra of the CH_2O(aq) solution are shown before (green crosses) and during (red circles) exposure to SO_2.

addition, lower intensity peaks are seen at 2785, 2870, and 2995 cm^{-1}. The resultant fits to the ssp-polarization spectra of CH_2O are shown as solid lines in Figures 2 and 3.

We attribute the small, broad peak at 3050 cm^{-1} to either the MG−OH stretching mode or an enhancement in the overall water binding environment. The main feature in the CH stretch region, a relatively sharp peak at 2910 cm^{-1}, is assigned to the MG CH_2 symmetric stretch mode, consistent with aqueous Raman measurements.[39,41] The remaining weak modes are attributed to nonfundamental modes of MG and contributions from other longer chain oligomers. Approximate assignments for these peaks are based on previous spectral assignments from bulk and surface studies of similar compounds; more specific spectral assignments are notoriously difficult due to the complex nature of their behavior in aqueous systems.[39,43,106]

The sps-polarization spectra, which reflect vibrational components in the plane of the surface (Figure 3b,d), closely resemble that of the neat vapor/water interface, except for the low-intensity peaks below 3000 cm^{-1}. We attribute the intensity in this spectral region to CH stretch modes. More specific assignments are unreasonable due to the low signal level and the inconsistency of previous assignments for formaldehyde in bulk solution.[39−44,106] Nonetheless, the peak parameters determined through these fits provide a baseline for assessing the changes to the spectral region when SO_2 is flowing over the surface. The perturbations due to exposure to SO_2 will be the focus of the following discussion.

Uptake of SO_2 to CH_2O(aq). *A Preview of the Results.* Figure 4 shows the VSF response from the formaldehyde-containing solution in the presence (red circles) and absence (green crosses) of flowing SO_2. Lowering the temperature from 23 (a,b) to 0 °C (c,d) has a significant impact in both the sps- and ssp-polarization schemes. Visual inspection suggests that the presence of SO_2 results in changes to the surface properties, but further spectral analysis is necessary to better understand these effects.

Similar to the analysis for CH_2O in Figure 3, a fit to eq 3 was used to determine parameters to understand the nature of the spectral perturbations due to SO_2. There are two primary differences between these spectra (Figure 4a−d) and those observed for the pre-exposed formaldehyde solution (Figure 3): (1) broadening of the free OH peak, which indicates that surface complexes are forming with water while SO_2 is flowing,[35−37] and (2) a change in the shape of the CH stretching region that is enhanced at 0 °C. Notably, the CH stretch region can no longer be fit using the parameters for the unexposed formaldehyde solution, suggesting that new species may be forming in the interfacial region.

There are several plausible explanations for the changes to the CH region: SO_2 may be complexing to CH_2O(aq) at the surface; the new peaks may be due to the reaction product, HMS; or a new surface complex may be forming between SO_2 and the HMS formed in solution (eq 2). To understand the nature of these changes, it is necessary to examine the surface spectroscopic response after removal of SO_2, as well as to measure the VSF response from a solution of HMS.

Figure 5 shows VSF spectra taken after exposing the formaldehyde-containing solution in Figure 3 to SO_2 (blue triangles). The spectra of the CH_2O containing surface before (green crosses) and during (red circles) exposure are shown for comparison. Consistent with the spectra in Figures 3 and 4, these spectra were acquired at room temperature (a,b) and 0 °C (c,d) using the (a,c) ssp- and (b,d) sps-polarization from spectra of unexposed formaldehyde surfaces (Figure 3) or those taken while flowing SO_2 (Figure 4). For example, in the sps-polarization, strong signal from the C−H modes is observed during exposure, but these peaks are greatly diminished after the removal of SO_2. As was seen for the formaldehyde-free solution, a surface complex between H_2O and SO_2 clearly forms, as indicated by the broadened free OH peak, with a return to a narrow free OH peak in the absence of SO_2. The similarity of the spectral response in these two spectral regions in the presence of SO_2 leads us to conclude that SO_2 also forms

dx.doi.org/10.1021/ja211632r | J. Am. Chem. Soc. 2012, 134, 9967−9977

a surface complex with an organic species at the surface. What that organic is, and its potential to form a surface SO_2 complex, are discussed in the next two sections.

Spectral Analysis of Aqueous HMS. As discussed earlier, HMS is a reaction product of H_2CO and SO_2. The surface spectroscopic response of an HMS solution demonstrates its presence at the surface, where it can further interact with SO_2. Figure 6 shows the VSF response of an aqueous HMS solution

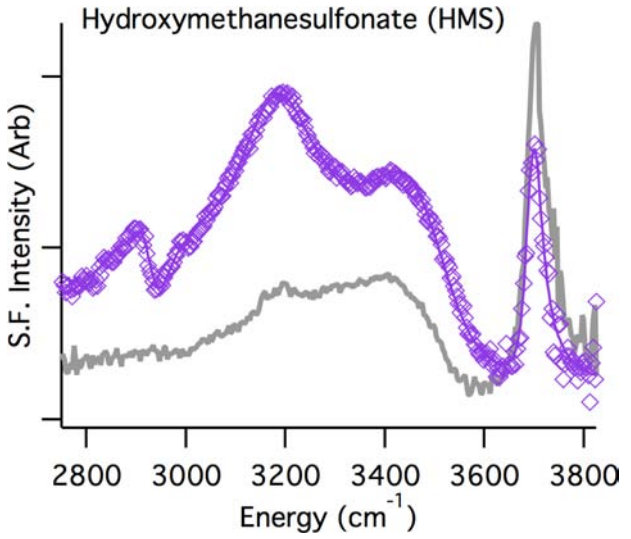

Figure 6. ssp-polarization spectrum of HMS (purple diamonds) compared to that of the vapor/water interface (gray). The thin solid line is the fit to the HMS spectrum. HMS was prepared by diluting formaldehyde to 3.2% w/v in saturated H_2SO_3(aq).

(purple diamonds) prepared by diluting a 16% w/v formaldehyde solution to 3.2% w/v in concentrated sulfurous acid (H_2SO_3); water is shown in gray for comparison. The equilibrium for this solution lies far to the right (eq 2); hence, we expect the primary components to be HMS and hydronium ions. The spectral response of the prepared HMS solution is very similar to that obtained after flowing SO_2 over a formaldehyde solution (Figure 5a). In fact, the prepared HMS solution and the solution that forms after flowing SO_2 gas over formaldehyde are fit using the same peak parameters, confirming that HMS is being produced by the uptake of SO_2 gas to aqueous formaldehyde. For both surfaces, the primary feature in the CH stretching region is a peak at ~2930 cm^{-1}, which we attribute to the CH_2 modes on HMS. The strong intensity in the coordinated water region observed for this HMS solution is consistent with the accumulation of hydronium and HMS ions in the interfacial region, as seen in previous sum frequency studies.[92,107,108]

Surface Complexation of SO_2 to HMS. The HMS solution has a pH of ~1, and is saturated in HSO_3^-. Therefore, additional SO_2 is unlikely to absorb and react in the bulk. As shown previously, flowing SO_2 over an acidic surface allows us to isolate spectral changes due to surface complexation from changes due to absorption and subsequent reaction.[37] The VSF spectra in Figure 7 show temporal changes to the surface response of the prepared HMS solution during (a,b) and after (c) the flow of SO_2. Spectra obtained while SO_2 is flowing (red circles) are compared to spectra obtained before (purple diamonds) and after (blue triangles) exposure to SO_2.

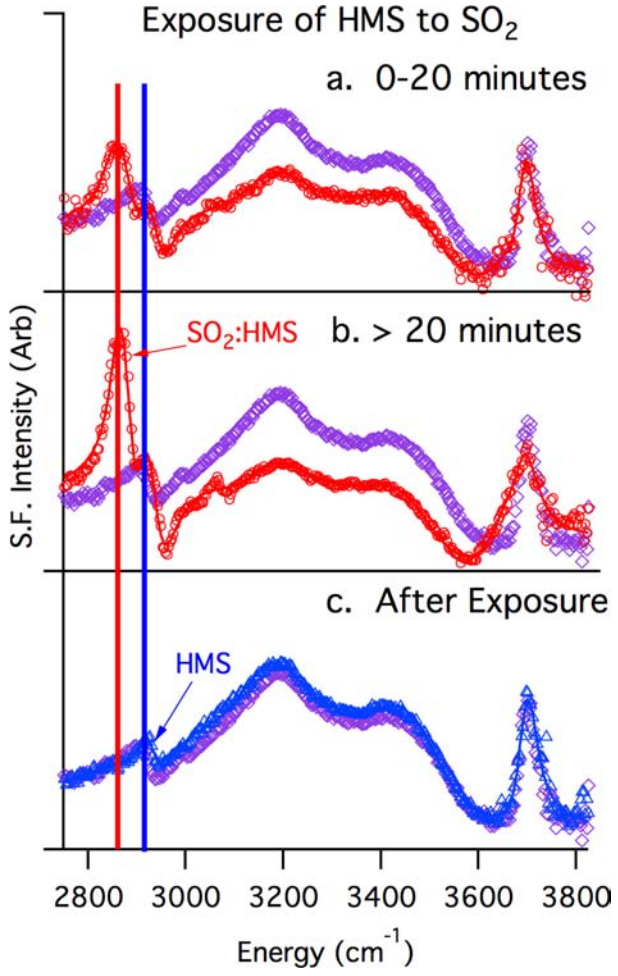

Figure 7. Surface spectrum of HMS during (red circles) and after (blue triangles) exposure to SO_2: (a) first 20 min of exposure; (b) 20–90 min of exposure; and (c) after removal of SO_2. The unexposed HMS surface (purple diamonds) is shown for comparison.

While SO_2 is flowing, two CH peaks are observed in the ssp-polarization scheme: the HMS peak at 2930 cm^{-1} and a peak at 2880 cm^{-1}. Notably, these same peaks are observed during the flow of SO_2 over the 3.2% w/v CH_2O solutions (Figure 4a,c). Thus, the peak at 2880 cm^{-1} is attributed to surface complexation between SO_2 and HMS and labeled (SO_2:HMS) in Figure 7. Both peaks grow in intensity with longer exposure to SO_2 (Figure 7b), suggesting that longer exposure to SO_2 causes more HMS to migrate to the interfacial region. Upon removal of SO_2, the interface returns to its initial state, and spectra obtained before and after exposure of HMS to SO_2 are nearly identical (Figure 7c), indicating that the surface changes in the presence of SO_2 are reversible and require the flow of SO_2. As with the free OH peak, complexation of SO_2 to HMS causes a red shift in the HMS peak at 2930 cm^{-1}. VSF spectra of a more concentrated CH_2O solution support this picture and confirm that the observed changes are primarily due to surface interactions between SO_2 and HMS, not CH_2O.

Exposure of CH_2O to SO_2: Time Evolution. Now that the spectral features indicative of the SO_2:HMS surface complexation have been established, we return to studies of the exposure of a CH_2O solution to SO_2. Figure 8 shows how the VSF response from a 16% w/v CH_2O solution evolves with

dx.doi.org/10.1021/ja211632r | J. Am. Chem. Soc. 2012, 134, 9967–9977

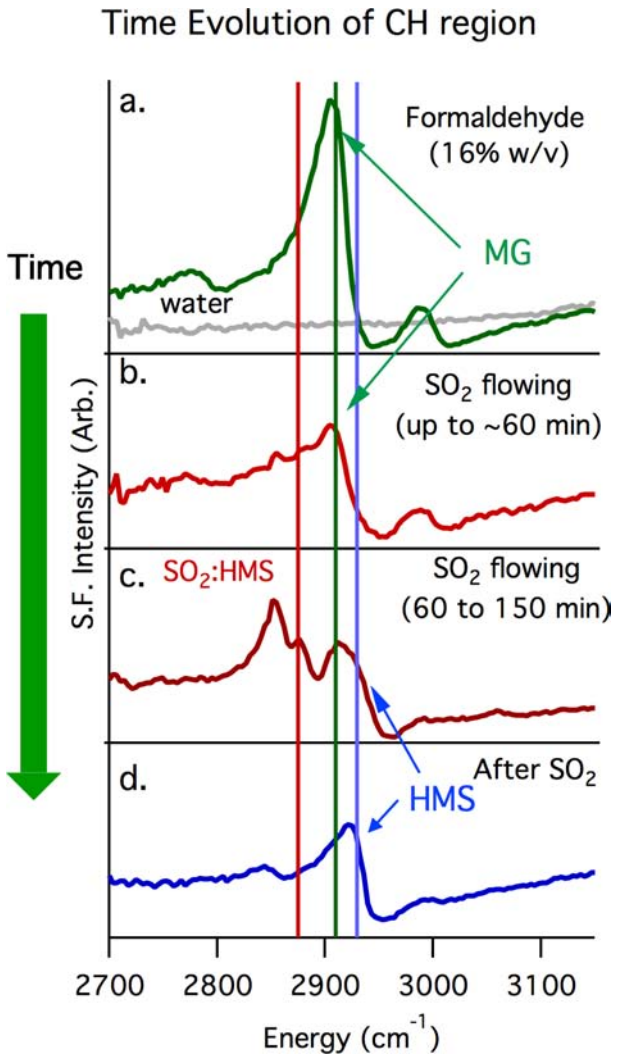

Figure 8. ssp-polarization spectra of 16% w/v formaldehyde: (a) formaldehyde (no SO_2); (b) up to 60 min of SO_2 exposure; (c) 60–150 min SO_2 exposure; and (d) after SO_2 exposure.

increased time of exposure to SO_2. As shown via the fits to the concentration series in Figure 2, the VSF response for the 16% w/v CH_2O solution can be fit to the same peaks as for the 3.2% w/v solution, indicating that the surface species are the same at both concentrations. However, at this higher concentration, the evolution of the CH stretch region can be observed as a function of SO_2 exposure time, because it takes longer to reach equilibrium. Each spectrum takes approximately 18 min to acquire. The broadening observed in the free OH region occurs almost immediately upon exposure to SO_2. Thus, only the CH stretch regions are shown Figure 8.

Prior to SO_2 exposure (Figure 8a), the primary feature is the formaldehyde CH stretch peak labeled as MG at 2910 cm^{-1}. Figure 8b shows the first hour of SO_2 exposure, during which the main MG CH peak loses intensity but does not shift position. The decrease in the intensity at 2910 cm^{-1} without a shift in frequency is consistent with a reduction in the amount of CH_2O at the surface due to the reaction between CH_2O and HSO_3^-. The possibility of a surface reaction to produce HMS cannot be ruled out, but there are no new spectral features to show evidence of a unique surface interaction. Figure 8c is an average of spectra taken during the second hour of exposure, showing that the CH peaks shift, and remain shifted, during subsequent exposure to SO_2. Two peaks appear as the formaldehyde reacts: the HMS–CH_2 stretch at ~2930 cm^{-1} and a new peak at ~2880 cm^{-1}. That the peak at ~2880 cm^{-1} is only observed after prolonged SO_2 exposure is consistent with the previous assignment to a complex between SO_2 and HMS. After the removal of SO_2, the dominant feature in this region is the peak at ~2930 cm^{-1}, which, as discussed previously, is attributed to the CH_2 mode of HMS that partitions to the interface. The surface spectra evolve over a relatively long time period, and in a two-step process, implying that the formation of HMS through the reaction between formaldehyde and SO_2 occurs primarily in the bulk.

Exposure of CH_2O to SO_2: Temperature Effects. As shown in Figure 4c,d, when the cold solutions are exposed to SO_2 gas (red circles), the spectral perturbations are much more dramatic than those observed at room temperature. Both the ssp- and sps-polarization spectra show significant changes in comparison to the unexposed CH_2O(aq) surfaces, as well as in comparison to spectra obtained at room temperature (Figure 4a,b). A significantly larger response is observed in the CH stretching region for both HMS and HMS–SO_2, as is a much broader peak in the free OH region.

Figure 9 highlights the CH stretching region from Figure 4c,d at this lower temperature, providing an overlay of spectra

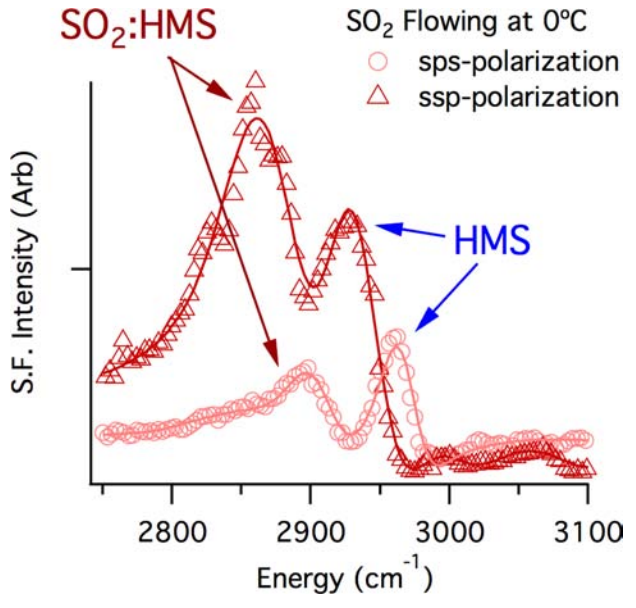

Figure 9. Comparison of spectra taken in the ssp- and sps-polarization schemes while SO_2 is flowing at 0 °C. Solid lines are fits.

taken in the ssp- (triangles) and sps-polarization (circles) schemes. The solid lines are fits to the data. The spectra shown here represent the interfacial region after 30–90 min of SO_2 exposure. At the colder temperature, the intensities of the CH peaks for HMS and HMS–SO_2 increase with time. Notably, the frequencies of the CH peaks change within the first 15 min of exposure, whereas the changes observed for the 16% w/v CH_2O solutions required over 60 min of SO_2 exposure.

The larger intensity changes at lower temperature help to clarify the spectral assignments. Both the ssp- and sps-polarization spectra give rise to two main peaks in the CH-stretching region. Consistent with experiments conducted at room temperature, the peaks at ~2930 (ssp) and ~2970 cm^{-1} (sps) are assigned to the CH_2 stretching modes from HMS.

dx.doi.org/10.1021/ja211632r | J. Am. Chem. Soc. 2012, 134, 9967–9977

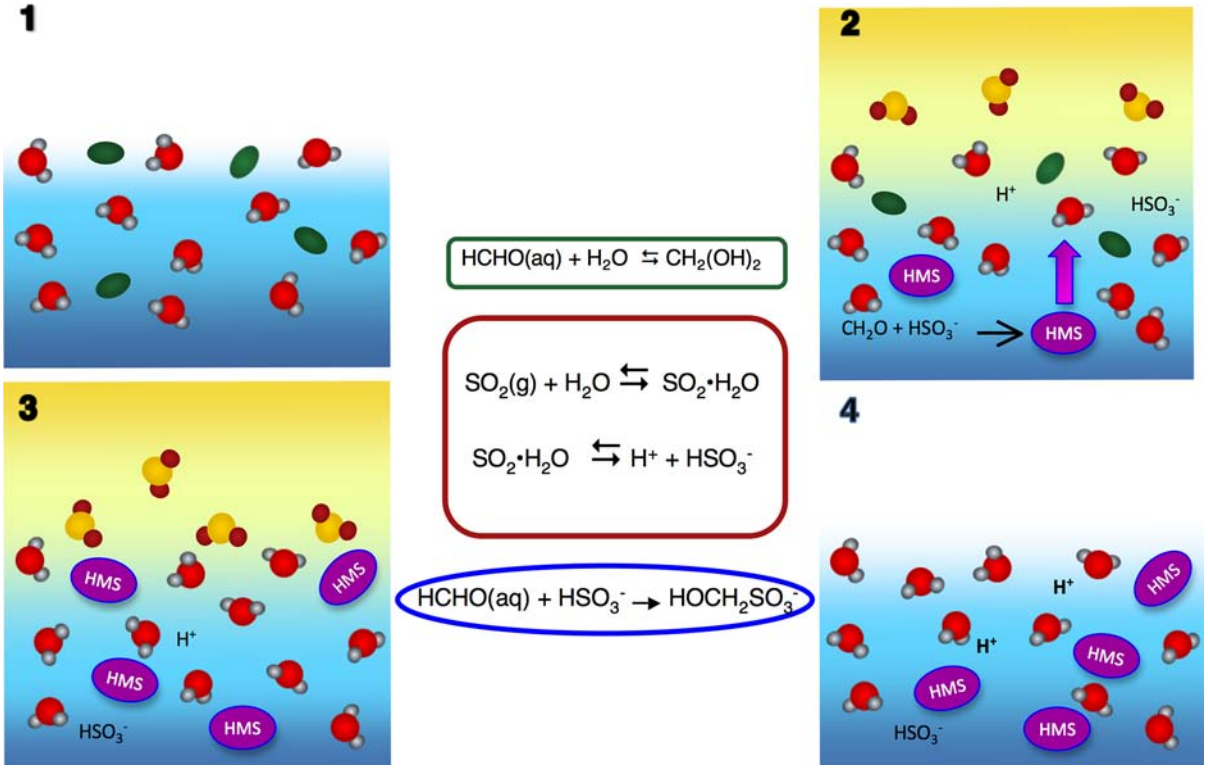

Figure 10. Cartoon depiction of the evolution of aqueous formaldehyde with SO_2 exposure over time: (1) Vapor/CH_2O(aq) interface. (2) Exposure to SO_2 results in surface complexes with water, and bulk reaction to form HMS. (3) Extended exposure to SO_2 results in surface complexes between SO_2 and HMS. (4) Surface complexes are reversible, but the ions formed during SO_2 exposure remain in solution.

The peaks at 2910 (ssp) and 2980 cm^{-1} (sps) are assigned to surface-adsorbed HMS complexing to SO_2, which red-shifts the HMS-CH_2 stretching frequencies in a manner analogous to the red-shifting of the free OH upon complexation of water to SO_2.[37] Similar peak parameters can be applied to fit spectra at both room temperature and 0 °C, but the intensities at the lower temperature are much higher. This intensity change is attributed to an increase in the HMS concentration at the surface caused by complexation with SO_2 and water in the interfacial region.

In both polarizations, lowering the temperature causes the magnitude and breadth of the complexed free OH peak to increase in a manner similar to what is observed for SO_2 at the vapor/water interface.[37] Analysis of the spectral changes in the free OH peak upon SO_2 bonding at the vapor/water interface shows that, although at room temperature only a fraction of the free OH bonds at the surface form a surface complex with flowing SO_2, at 0 °C nearly all free OH modes are involved in SO_2 surface complexation.[37] Computational studies suggest that the surface complex is comprised of SO_2 bound to several surface water molecules, largely through the sulfur atom of SO_2.[109] For the formaldehyde solution at 0 °C, the increased breadth and magnitude of the free OH peak in the presence of SO_2 is even larger than observed at the vapor/water interface. For the formaldehyde solution at 0 °C, in the ssp-polarization scheme the high-energy region can be fit either using a single broad peak at 3630 cm^{-1} or with two peaks, a narrower peak at 3660 cm^{-1} and a broad peak at 3580 cm^{-1}, similar to what has been discussed previously for SO_2 at the vapor/water interface.[37] Given the high concentration of surface SO_2 at cold temperatures and its ability to induce more HMS to the surface, it is likely that the two effects act in concert to form a mixture of ions and HMS−SO_2−H_2O surface complexes in the interfacial region.

Accompanying the two large spectral changes at the low and high regions of the spectra in Figure 4c,d at 0 °C is a corresponding drop in signal from in the intensity in the 3000−3500 cm^{-1} region, attributed to interfacial water molecules with strong to moderately strong hydrogen bonds. This is very different from what is observed for SO_2 at the neat vapor/water interface, where such a drop is absent. These changes are consistent with a reduced electric field due to the accumulation of HMS and associated ions at the surface while the SO_2 is flowing.

As has been seen in previous VSF studies,[35,89,92,110−114] with a decreased electric field the net orientation of these H-bonded interfacial water molecules is reduced, with a consequential reduction of the VSF signal in the signature 3000−3500 cm^{-1} region. This reduction in the more strongly bonded water molecules results from an increase in the number of loosely coordinated waters and those involved in solvating ions, whose spectral signatures generally lie in the 3600−3700 cm^{-1} region.[35,89] Hence, we attribute the increase in intensity that we see in this region during SO_2 flow, and in the presence of surface HMS, to solvating water molecules involved in the HMS−SO_2 surface complexes within the topmost interfacial layers. As a relatively large, polarizable compound, HMS has the potential to hydrogen-bond with water or sulfite molecules in many different configurations in solution. However, at the interface these binding possibilities are much more limited, an interpretation supported by the narrowing of the CH peaks of HMS observed, relative to those measured after removing SO_2, when the ions are once again more solvated.

dx.doi.org/10.1021/ja211632r | J. Am. Chem. Soc. 2012, 134, 9967−9977

The picture that has emerged from these results is as follows. SO_2 adsorbs to the vapor/CH_2O(aq) interface and forms a surface complex with water molecules in the topmost interfacial region. This is followed by absorption of the SO_2 into the bulk to form HSO_3^-. The resultant HSO_3^- ions react with CH_2O(aq) to form HMS. HMS migrates to the surface, where it bonds to surface-adsorbed SO_2, facilitating the reversible accumulation of HMS at the surface (Figure 7a). With increased SO_2 exposure time, the concentration of HMS complexed to SO_2 at the surface increases, as manifested by an increase in the intensity of the peaks in the CH region (Figure 7b). Lowering the temperature causes even further SO_2–HMS complex formation and subsequent enhancement of these changes. When the flow of SO_2 is stopped, the surface complexes between SO_2 and HMS fall apart, and the resulting spectra are indistinguishable from those of an unexposed HMS solution.

CONCLUSIONS

These surface spectroscopic studies highlight the influence of surface-adsorbed SO_2 on the behavior of solutions containing both SO_2 and CH_2O. The cartoon in Figure 10 provides a simple illustration of the interfacial behavior observed in these experiments. The aqueous formaldehyde solution shows evidence of surface-bound organic species, largely in the methylene glycol form, depicted as green ovals in Figure 10. Upon exposure to SO_2, the surface water molecules immediately form complexes with surface-bound SO_2, facilitating absorption and reaction with water to form HSO_3^-. The subsequent reaction between CH_2O and HSO_3^- to form HMS occurs primarily in the bulk solution, depleting surface-adsorbed formaldehyde concentrations. HMS migrates toward the interfacial region, where it forms surface complexes with SO_2; possibly facilitated by the SO_2–H_2O complex found at the vapor/water interface.[35−37,115] Notably, exposure to SO_2 results in an increase in the HMS concentration at the surface. Similar to the complexes between water and SO_2, the HMS–SO_2 complexes are reversible, and are only observed while the SO_2 gas is flowing over the surface. But these surface species, particularly at lower temperatures, have a profound influence on water structure and appear to decrease the level of overall coordination and orientation in the interfacial region.

Cooling the formaldehyde solution to an atmospherically relevant temperature results in a significant enhancement in the adsorption of SO_2 to surface water and HMS. This leads to a structurally more congested interface where the orientations of the surface complexes between SO_2 and HMS are more constrained. This is consistent with the increased contribution from loosely coordinated water molecules in the topmost surface region. The main spectral contributions from water are from either water molecules that are involved in complexes to SO_2 or those with weak hydrogen-bonding interactions with other waters. This points to an interface that is mainly populated by surface-bound organics, ions, and other species that are loosely solvated by water. These surface species are short-lived, and the ions return to solution when the SO_2 is removed from the system. The resultant solution exhibits enhanced interfacial coordination consistent with spectra of other low-pH, ion-containing solutions.

These results highlight the significance of interfacial chemistry in the atmosphere, particularly as it pertains to the uptake of gaseous pollutants such as SO_2 onto organic containing water surfaces. It has long been recognized that organic pollutants persist in the atmosphere, where they can adsorb on particle surfaces, playing an important role in aqueous surface chemistry. However, few studies have been able to directly probe the nature of these interactions. Organic species have the potential to act as a barrier to gas uptake, but this study shows that some organics can act as magnets for gas adsorption. In addition, these experiments demonstrate that the low temperature conditions of the lower atmosphere are likely to further enhance the formation of such surface complexes in the presence and absence of organics. Evidence that water-soluble organic species can complex to atmospheric gases during the uptake process has important implications for atmospheric chemistry. Once surface complexes are formed they are ideally positioned for photochemical processing or reaction with other species in the gas phase, increasing the number of available reaction pathways in comparison to those available in the bulk. From these experiments, it is clear that gas uptake is a multifaceted process in which the surface plays an essential role.

AUTHOR INFORMATION

Corresponding Author

richmond@uoregon.edu

Notes

The authors declare no competing financial interest.

ACKNOWLEDGMENTS

The authors thank the National Science Foundation (CHE 0652531) for supporting this research.

REFERENCES

(1) Blando, J. D.; Turpin, B. J. *Atmos. Environ.* **2000**, *34*, 1623−1632.
(2) Vaden, T. D.; Song, C.; Zaveri, R. A.; Imre, D.; Zelenyuk, A. *PNA* **2010**, *107*, 6658−6663.
(3) Iraci, L. T.; Tolbert, M. A. *J. Geophys. Res.* **1997**, *102*, 16099−16107.
(4) Davidovits, P.; Kolb, C. E.; Wiliams, L. R.; Jayne, J. T.; Worsnop, D. R. *Chem. Rev.* **2006**, *106*, 1323−1354.
(5) Whiteaker, J. R.; Prather, K. A. *Atmos. Environ.* **2003**, *37*, 1033−1043.
(6) Kroll, J. H.; Ng, N. L.; Murphy, S. M.; Varutbangkul, V.; Flagan, R. C.; Seinfeld, J. H. *J. Geophys. Res.* **2005**, *110*, D23207/1−D23207/10.
(7) Russell, L. M.; Maria, S. F.; Myneni, S. C. B. *Geophys. Res. Lett.* **2002**, *29*, 1779/1−1779/4.
(8) Hatch, L. E.; Creamean, J. M.; Ault, A. P.; Surratt, J. D.; Chan, M. N.; Seinfeld, J. H.; Edgerton, E. S.; Su, Y.; Prather, K. A. *Environ. Sci. Technol.* **2011**, *45*, 5105−5111.
(9) Solomon, S.; Qin, D.; Manning, M.; Alley, R. B.; Bernsten, T.; Bindoff, N. L.; Chen, Z.; Chidthaisong, A.; Gregory, J. M.; Hegeri, G. C.; Heimann, M.; Hewitson, B.; Hoskins, B. J.; Joos, F.; Jouzei, H.; Kattsov, V.; Lohmann, U.; Matsuno, T.; Molina, H.; Nicholls, N.; Overpeck, J.; Raga, G.; Ramaswamy, V.; Ren, J.; Rusticucci, M.; Somerville, R.; Stocker, T. F.; Whetton, P.; Wood, R. A.; Wratt, D. In *Climate Change 2007: The Physical Basis. Contribution of Working Group I to the Fourth Assessment Report of the Intergovernmental Panel on Climate Change*; Solomon, S., Qin, D., Manning, M., Chen, Z., Marquis, K. B., Averyt, K. B., Tignor, M., Miller, H. L., Eds.; Cambridge University Press: Cambridge, UK/New York, 2007.
(10) Prenni, A. J.; De Mott, P. J.; Kreidenweis, S. M.; Sherman, D. E.; Russell, L. M.; Ming, Y. *J. Phys. Chem. A* **2001**, *105*, 11240−11248.
(11) Bilde, M.; Svenningsson, B.; Mønster, J.; Rosenørn, T. *Environ. Sci. Technol.* **2003**, *37*, 1371−1378.
(12) Kim, H. I.; Goddard, W. A. I.; Beauchamp, J. L. *J. Phys. Chem. A* **2006**, *110*, 7777−7786.

(13) Grunwald, E.; Pan, K.-C.; Effio, A. *J. Phys. Chem.* **1976**, *80*, 2937−2940.
(14) Beyer, K. D.; Friesen, K.; Bothe, J. R.; Palet, B. *J. Phys. Chem. A* **2008**, *112*, 11704−11713.
(15) Clegg, S. L.; Seinfeld, J. H. *J. Phys. Chem. A* **2006**, *110*, 5718−5734.
(16) Rosado-Reyes, C. M.; Francisco, J. S. *J. Phys. Chem. A* **2006**, *110*, 4419−4433.
(17) Freedman, M. A.; Hasenkopf, C. A.; Beaver, M. R.; Tolbert, M. A. *J. Phys. Chem. A* **2009**, *113*, 13584−13592.
(18) Choi, M. Y.; Chan, C. K. *Environ. Sci. Technol.* **2002**, *36*, 2422−2428.
(19) Jacobson, M. C.; Hansson, H. C.; Noone, K. J.; Charlson, R. J. *Rev. Geophys.* **2000**, *38*, 267−294.
(20) Ming, Y.; Russell, L. M. *J. Geophys. Res.* **2004**, *109*, D10206/1−D10206/14.
(21) Stephanou, E. G. *Nature* **2005**, *434*, 31.
(22) Maria, S. F.; Russell, L. M.; Gilles, M. K.; Myneni, S. C. B. *Science* **2004**, *306*, 1921−1924.
(23) Goss, K.-U. *J. Phys. Chem. A* **2009**, *113*, 12256−12259.
(24) Ellison, G. B.; Tuck, A. F.; Vaida, V. *J. Geophys. Res.* **1999**, *104*, 11633−11641.
(25) Hyvärinen, A.-P.; Raatikainen, T.; Laaksonen, A.; Viisanen, Y.; Lihavainen, H. *Geophys. Res. Lett.* **2005**, *32*, L16806.
(26) Eliason, T. L.; Gilman, J. B.; Vaida, V. *Atmos. Environ.* **2004**, *38*, 1367−1378.
(27) Molina, M. J.; Ivanov, A. V.; Trakhtenberg, S.; Molina, L. T. *Geophys. Res. Lett.* **2004**, *31*, L22104−1−L22104−5.
(28) O'Dowd, C. D.; Facchini, M. C.; Cavalli, F.; Ceburnis, D.; Decesari, S.; Fuzzi, S.; Yoon, J. J.; Putaud, J.-P. *Nature* **2004**, *431*, 676−680.
(29) Donaldson, D. J.; Vaida, V. *Chem. Rev.* **2006**, *106*, 1445−1461.
(30) Bluhm, H.; Siegmann, H. C. *Surf. Sci.* **2009**, *603*, 1969−1978.
(31) Fuzzi, S.; Andreae, M. O.; Huebert, B. J.; Kulmala, M.; Bond, T. C.; Boy, M.; Doherty, S. J.; Guenther, A.; Kanakidou, M.; Kawamura, K.; Kerminen, V.-M.; Lohmann, U.; Russell, L. M.; Pöschl, U. *Atmos. Chem. Phys. Discuss.* **2005**, *5*, 11729−11780.
(32) Rudich, Y. *Chem. Rev.* **2003**, *103*, 5097−5124.
(33) Rudich, Y.; Donahue, N. M.; Mentel, T. F. *Annu. Rev. Phys. Chem.* **2007**, *58*, 321−352.
(34) Valsaraj, K. T.; Thibodeaux, L. J. *J. Phys. Chem. Lett.* **2010**, *1*, 1694−1700.
(35) Tarbuck, T. L.; Richmond, G. L. *J. Am. Chem. Soc.* **2006**, *128*, 3256−3267.
(36) Tarbuck, T. L.; Richmond, G. L. *J. Am. Chem. Soc.* **2005**, *127*, 16806−16807.
(37) Ota, S. T.; Richmond, G. L. *J. Am. Chem. Soc.* **2011**, *133*, 7497−7508.
(38) Barret, M.; Houdier, S.; Domine, F. *J. Phys. Chem. A* **2011**, *115*, 307−317.
(39) Lebrun, N.; Dhamelincourt, P.; Focsa, C.; Chazallon, B.; Destombes, J. L.; Prevost, D. *J. Raman Spectrosc.* **2003**, *34*, 459−464.
(40) Hibben, J. *J. Am. Chem. Soc.* **1931**, *53*, 2418.
(41) Chazallon, B.; Oancea, A.; Capoen, B.; Focsa, C. *Phys. Chem. Chem. Phys.* **2008**, *10*, 702−712.
(42) Chazallon, B.; Lebrun, N.; Dhamelincourt, P.; Toubin, C.; Focsa, C. *J. Phys. Chem. B* **2005**, *109*, 432−439.
(43) Hanoune, B.; Paccou, L.; Delcroix, P.; Guinet, Y. *J. Raman Spectrosc.* **2011**, *42*, 1202−1204.
(44) Ryabova, R. S.; Voloshenko, G. I.; Maiorov, V. D.; Osipova, G. F. *Russ. J. Appl. Chem.* **2002**, *75*, 22−24.
(45) Jayne, J. T.; Worsnop, D. R.; Kolb, C. E.; Swartz, E.; Davidovits, P. *J. Phys. Chem.* **1996**, *100*, 8015−8022.
(46) Swartz, E.; Boniface, J.; Tchertkov, I.; Rattigan, O. V.; Robinson, D. V.; Davidovits, P.; Worsnop, D. R.; Jayne, J. T.; Kolb, C. E. *Environ. Sci. Technol.* **1997**, *31*, 2634−2641.
(47) Dimitrova, Y. *J. Mol. Struct. (Theochem)* **1997**, *391*, 251−257.
(48) Oancea, A.; Hanoune, B.; Focsa, C.; Chazallon, B. *Environ. Sci. Technol.* **2009**, *43*, 435−440.
(49) Jayne, J. T.; Duan, S. X.; Davidovits, P.; Worsnop, D. R.; Zahniser, M. S.; Kolb, C. E. *J. Phys. Chem.* **1992**, *96*, 5452−5460.
(50) Albert, M.; Coto García, B.; Kreiter, C.; Maurer, G. *AIChE J.* **1999**, *45*, 2024−2033.
(51) Finlayson-Pitts, B. J.; Pitts, J. N., Jr. *Chemistry of the Upper and Lower Atmosphere*; Academic Press: San Diego, 2000.
(52) Boyce, S. D.; Hoffman, M. R. *J. Phys. Chem.* **1984**, *88*, 4740−4746.
(53) Munger, J. W.; Jacob, D. J.; Hoffman, M. R. *J. Atmos. Chem.* **1984**, *1*, 335−350.
(54) Munger, J. W.; Tiller, C.; Hoffman, M. R. *Science* **1986**, *231*, 247−249.
(55) Warneck, P. *J. Atmos. Chem.* **1989**, *8*, 99−117.
(56) Ang, C. C.; Lipari, F.; Swarin, S. J. *Environ. Sci. Technol.* **1987**, *21*, 102−105.
(57) Olson, T. M.; Hoffman, M. R. *Atmos. Environ.* **1989**, *23*, 985−997.
(58) Munger, J. W.; Jacob, D. J.; Waldman, J. M.; Hoffman, M. R. *J. Geophys. Res.* **1983**, *88*, 5109−5121.
(59) Richmond, G. L. *Chem. Rev.* **2002**, *102*, 2693−2724.
(60) Bloembergen, N. *Nonlinear Optics*; W. A. Benjamin, Inc.: New York, 1965.
(61) Vidal, F.; Tadjeddine, A. *Rep. Prog. Phys.* **2005**, *68*, 1095−1127.
(62) Buck, M.; Himmelhaus, M. *J. Vac. Sci. Technol., A* **2001**, *19*, 2717−2736.
(63) Hemminger, J. C. *Int. Rev. Phys. Chem.* **1999**, *18*, 387−417.
(64) Lambert, A. G.; Davies, P. B.; Neivandt, D. J. *Appl. Spectrosc. Rev.* **2005**, *40*, 103−145.
(65) Guyot-Sionnest. *Surf. Sci.* **2005**, *585*, 1−2.
(66) Voges, A. B.; Al-Abadleh, H. A.; Geiger, F. M. In *Environmental Catalysis*; Grassian, V. H., Ed.; Taylor and Francis: Boca Raton, FL, 2005.
(67) Rao, Y.; Song, D.; Turro, N. J.; Eisenthal, K. B. *J. Phys. Chem. B* **2008**, *112*, 13572−13576.
(68) Bloembergen, N. *Opt. Acta* **1966**, *13*, 311−322.
(69) Ji, N.; Ostroverkhov, V.; Shiu, Y.-J.; Shen, Y.-R. *J. Am. Chem. Soc.* **2006**, *128*, 8845−8848.
(70) Shen, Y. R.; Ostroverkhov, V. *Chem. Rev.* **2006**, *106*, 1140−1154.
(71) Ishibashi, T.-A.; Onishi, H. *Appl. Spectrosc.* **2002**, *56*, 1298−1302.
(72) Ostroverkhov, V.; Waychunas, G. A.; Shen, Y. R. *Phys. Rev. Lett.* **2005**, *94*, 046102/1−046102/4.
(73) Shen, Y. R. *Pure Appl. Chem.* **2001**, *73*, 1589−1598.
(74) Miranda, P. B.; Shen, Y. R. *J. Phys. Chem. B* **1999**, *103*, 3292−3307.
(75) Hirose, C.; Akamatsu, N.; Domen, K. *Appl. Spectrosc.* **1992**, *46*, 1051−1072.
(76) Fourkas, J. T.; Walker, R. A.; Can, S. Z.; Gershgoren, E. *J. Phys. Chem. C* **2007**, *111*, 8902−8915.
(77) Zhu, X. D.; Suhr, H.; Shen, Y. R. *Phys. Rev. B* **1987**, *35*, 3047−3049.
(78) Bloembergen, N.; Pershan, P. S. *Phys. Rev.* **1962**, *128*, 606−622.
(79) Shen, Y. R. *Nature* **1989**, *337*, 519−525.
(80) Bain, C. D. *J. Chem. Soc., Faraday Trans.* **1995**, *91*, 1281−1296.
(81) Löbau, J.; Wolfrum, K. *J. Opt. Soc. Am. B* **1997**, *14*, 2505−2512.
(82) McGall, S. J.; Davies, P. B.; Neivandt, D. J. *J. Phys. Chem. B* **2004**, *108*, 16030−16039.
(83) Bain, C. D.; Davies, P. B.; Ong, T. H.; Ward, R. N.; Brown, M. A. *Langmuir* **1991**, *7*, 1563−1566.
(84) Gragson, D.; McCarty, B.; Richmond, G. L.; Alavi, D. S. *J. Opt. Soc. Am. B* **1996**, *13*, 1075−2083.
(85) Gragson, D.; Alavi, D.; Richmond, G. L. *Opt. Lett.* **1995**, *20*, 1991−1993.
(86) Allen, H. C.; Raymond, E. A.; Richmond, G. L. *J. Phys. Chem. A* **2001**, *105*, 1649−1655.
(87) Raymond, E. A.; Tarbuck, T. L.; Brown, M. G.; Richmond, G. L. *J. Phys. Chem. B* **2003**, *107*, 546−556.

(88) Raymond, E. A.; Tarbuck, T. L.; Richmond, G. L. *J. Phys. Chem. B* **2002**, *106*, 2817−2820.
(89) Raymond, E. A.; Richmond, G. L. *J. Phys. Chem. B* **2004**, *108*, 5051−5059.
(90) Walker, D. S.; Hore, D. K.; Richmond, G. L. *J. Phys. Chem. B* **2006**, *110*, 20451−20459.
(91) Walker, D. S.; Richmond, G. L. *J. Phys. Chem. C* **2007**, *111*, 8321−8330.
(92) Tarbuck, T. L.; Ota, S. T.; Richmond, G. L. *J. Am. Chem. Soc.* **2006**, *128*, 14519−14527.
(93) Auer, B. M.; Skinner, J. L. *J. Chem. Phys.* **2008**, *129*, 214705/1−214705/14.
(94) Tian, C.-S.; Shen, Y. R. *J. Am. Chem. Soc.* **2009**, *131*, 2790−2791.
(95) Tian, C. S.; Shen, Y. R. *Chem. Phys. Lett.* **2009**, *470*, 1−6.
(96) Fan, Y.; Chen, X.; Yang, L.; Cremer, P. S.; Gao, Y. Q. *J. Phys. Chem. B* **2009**, *113*, 11672−11679.
(97) Sovago, M.; Vartiainen, E. M.; Bonn, M. *J. Phys. Chem. C* **2009**, *113*, 6100−6106.
(98) Auer, B. M.; Skinner, J. L. *J. Phys. Chem. B* **2009**, *113*, 4125−4130.
(99) Sovago, M.; Campen, R. K.; Bakker, H. J.; Bonn, M. *Chem. Phys. Lett.* **2009**, *470*, 7−12.
(100) Sovago, M.; Campen, R. K.; Wurpel, G. W. H.; Müller, M.; Bakker, H. J.; Bonn, M. *Phys. Rev. Lett.* **2008**, *100*, 173901/1−173901/4.
(101) Auer, B. M.; Skinner, J. L. *Chem. Phys. Lett.* **2009**, *470*, 13−20.
(102) Bakker, H. J.; Skinner, J. L. *Chem. Rev.* **2010**, *110*, 1498−1517.
(103) Buch, V. *J. Phys. Chem. B* **2005**, *109*, 17771−17774.
(104) Dang, L. X.; Chang, T.-M. *J. Chem. Phys.* **1997**, *106*, 8149−8159.
(105) Feng, R.-r.; Guo, Y.; Lü, R.; Velarde, L.; Wang, H.-f. *J. Phys. Chem. A* **2011**, *115*, 6015−6027.
(106) Begue, D.; Elissalde, S.; Pere, E.; Iratcabal, P.; Pouchan, C. *J. Phys. Chem. A* **2006**, *110*, 7793−7800.
(107) Levering, L. M.; Sierra-Hernández; Allen, H. C. *J. Phys. Chem. C* **2007**, *111*, 8814−8826.
(108) Baldelli, S.; Schnitzer, C.; Shultz, M. J. *Chem. Phys. Lett.* **1999**, *302*, 157−163.
(109) Baer, M.; Mundy, C. J.; Chang, T.-M.; Tao, F.-M.; Dang, L. X. *J. Phys. Chem. B* **2010**, *114*, 7245−7249.
(110) Jungwirth, P.; Winter, B. *Annu. Rev. Phys. Chem.* **2008**, *59*, 343−366.
(111) Kolb, C. E.; Worsnop, D. R. *Annu. Rev. Phys. Chem.* **2012**, in press.
(112) Tian, C.; Byrnes, S. J.; Han, H.-L.; Shen, Y. R. *J. Phys. Chem. Lett.* **2011**, *2*, 1946−1949.
(113) Hua, W.; Jubb, A. M.; Allen, H. C. *J. Phys. Chem. Lett.* **2011**, *2*, 2515−2520.
(114) Schnitzer, C.; Baldelli, S.; Shultz, M. J. *J. Phys. Chem. B* **2000**, *104*, 585−590.
(115) Jayne, J. T.; Davidovits, P.; Worsnop, D. R.; Zahniser, M. S.; Kolb, C. E. *J. Phys. Chem.* **1990**, *94*, 6041−6048.